2023 IEEE/ASME International Conference on Advanced Intelligent Mechatronics (AIM)
June 28-30, 2023. Seattle, Washington, USA

Prototype of Ball-like Jumping Robot for Playful Learning

Yuto Sango and Hiroyuki Ishii, *Member, IEEE*

Abstract— **Free and structured play should be introduced to children during their childhood in a well-balanced manner. Balls may be used in both plays; therefore, we proposed ball-like robot which will provide children both types of plays. We focused on the jumping of the ball and developed a ball-like jumping robot. In this study, we reported the mechanical design, robot system, performance, and potential of the ball-like robot to jump continuously and turn right/left for controlling the jumping direction. The robot mainly consists of one vibration unit and two compressed springs. Two motions, jumping and turning, are generated by controlling rotation speed of eccentric motors constituting the vibration unit. The experimental results confirmed that the fabricated robot can control the jumping height and average turning angular velocity depending on the rotation speed of the eccentric motors. Furthermore, the robot can be controlled by an operator via commands from a computer with a short delay. The robot can move dynamically. We proposed applications for free and structured play using the ball-like robot from these results.**

I. Introduction

Childhood experiences and environmental influences have a significant impact on lifelong learning and behavior [1]. According to UNICEF, play is one of the most important ways in which young children gain essential knowledge and skills and experience [2]. This stimulation builds children's basic abilities for adults: cognitive skills, emotional well-being, social competence, and sound physical and mental health. Furthermore, diversity of play is necessary for children to discover what they are good at and what they like to do [3]. Therefore, "playful learning" is very important for children. The term "playful learning" is an umbrella term that is used to include free and more structured, guided play contexts, and games [4]. This is classified as free play (unstructured play) and structured play. Free play is child-led and purposeless play, whereas structured play is purposeful with adult intervention. These plays should be introduced in a well-balanced manner [5, 6]. However, free play has decreased today [3, 7]. One of the reasons is increment of passive play through television or computer/video games [7]. Therefore, we proposed a robot providing children various play based on free and structured play in a well-balanced manner.

In parent-child play, blocks, ball, mailbox, puppy, and door features elicited more interactions than other features [8]. Ball play enhances children's motor skills through kicking, throwing, rolling, and catching; therefore, ball play can be used in both free and structured play. Thus, we focused on a ball-like robot for play which is capable of two movements: rolling and bouncing (or jumping). Ball-like robot for play was developed mainly in rolling motion operated by remote control and autonomously [9-11]. Ball-like robot capable of jumping motion without autonomous operation has been developed as a toy (by SEGA TOYS CO., LTD). However, ball-like autonomously jumping robot has not been focused upon. Therefore, we developed it to widen the choice of play and expanding children's experience. Particularly, we incorporated continuous jumping into the robot to facilitate children with a smoother play experience.

In free play, the robot is treated as a real ball, and children play by autonomous movement of the robot. The robot should be soft, tough, and safe like a real ball. Parten [12] classified play into two types, solitary, and group. Therefore, in structured play, the robot activates children's motion through two scenarios, solitary, and group. The solitary scenario facilitates self-expression of a child by play between the robot and the child; the group scenario facilitates self-expression in addition to children interaction by the robot acting as a bridge of communication between children. In this study, we reported the mechanical design, robot system, performance, and potential of the ball-like robot capable of jumping continuously and turning right/left for changing jumping direction.

Continuous jumping robots are classified into two mechanisms. One is a shape changing mechanism, such as, pneumatic actuator [13], hydraulic actuator [14], and spring [15], while another is a vibration mechanism with eccentric motors [16-18]. The latter provides the robot capability of continuous jumping with unchanging shape, and is more suitable for ball-like robot as it requires maintenance of its ball shape.

The fabricated robot prototype is shown in Fig. 1 and its main specifications are shown in Table I. The robot is capable of continuous jumping, turning right/left, and being operated by a wireless control from a computer. These motions are operated by only one mechanism that comprises one vibration unit and two compression springs. It consists of an outer sphere assembled by two polyvinyl chloride (PVC) hemispheres, one vibration unit, two compressed springs with spring constant 4.9N/mm, one carbon fiber reinforced plastics (CFRP) shaft, inertial measurement unit (IMU), electronic circuit, and a three-cell Li-po battery. The vibration unit consists of two 1.6 W direct current (DC) motors, two eccentric 20 g weights with eccentricity 20 mm, battery, and electronic circuit. Main components of the vibration unit are made of polycarbonate (PC) for heat-resistance.

The rest of this paper is organized as follows: Section II and III describe mechanical design of the robot and the robot system, respectively; Section IV discusses the experiments

*This work was supported in part by the JSPS KAKENHI under Grants 19H01130, and 21H05055.

Yuto Sango is with Department of Modern Mechanical Engineering, Waseda University, Tokyo, Japan (e-mail: 35yuto@fuji.waseda.jp).

Hiroyuki Ishii is with Department of Modern Mechanical Engineering, Waseda University, and the Human Robotics Institute (HRI), Waseda University, Tokyo, Japan (e-mail: hiro.ishii@waseda.jp).

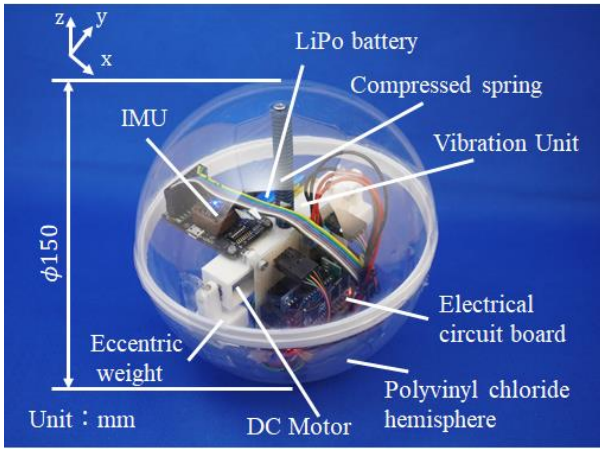

Figure 1. Prototype of the ball-like robot.

TABLE I. THE SPECIFICATION OF THE PROTYPE

Specification	Value
Size mm	150
Weight g	295
Max jumping height mm	15
Max average turning angular velocity rad/s	1.4

conducted to evaluate the robot performance; the results are discussed in Section V; finally, Section VI concludes this study.

II. Mechanical Design

A. Continuous Jumping Design

An overview of the continuous jumping mechanism is shown in Fig. 2. This comprises one vibration unit and two compressed springs. The vibration unit constitutes of two coaxially assembled DC motors with each encoder having of a shaft having eccentric weights. The vibration is generated by rotating each of the weight synchronously in the opposite directions at the same speed. In rotation of one eccentric weight, centrifugal force is described by

$$\begin{bmatrix} f_x \\ f_z \end{bmatrix} = m_w \varepsilon \left\{ \dot{\theta}_{(t)}^{\,2} \begin{bmatrix} \sin\theta_{(t)} \\ -\cos\theta_{(t)} \end{bmatrix} - \ddot{\theta}_{(t)} \begin{bmatrix} \cos\theta_{(t)} \\ \sin\theta_{(t)} \end{bmatrix} \right\}, \qquad (1)$$

where f_x and f_z, are centrifugal forces in x- and z-axis, respectively, m_w is mass of the eccentric weight, ε is eccentricity, and $\theta_{(t)}$ is angle of eccentric weights relative to negative z-axis. By rotating the coaxially assembled weights in the opposite directions, the x-axis force is canceled and only the z-axis force is retained. Therefore, vibration force is described by

$$\begin{bmatrix} F_x \\ F_z \end{bmatrix} = -2 m_w \varepsilon \begin{bmatrix} 0 \\ \dot{\theta}_{(t)}^{\,2} \cos\theta_{(t)} + \ddot{\theta}_{(t)} \sin\theta_{(t)} \end{bmatrix}, \qquad (2)$$

where F_x and F_z are vibration forces in x- and z-axis, respectively. Although the above model does not contain springs, the continuous jumping motion can be roughly grasped by focusing on the vibration force. Vibration force, as shown in (2), makes the two compressed springs vibrate, so that it stores elastic energy and results in jumping. Continuous jumping is caused by continuing vibration.

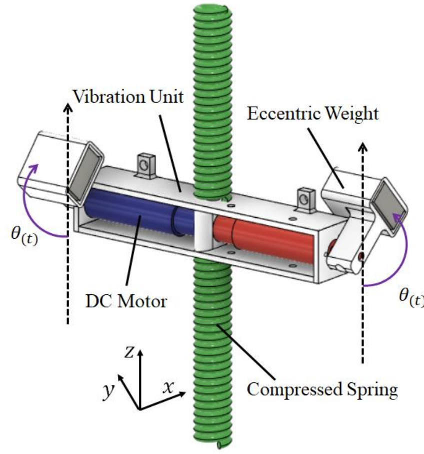

Figure 2. Continuous jumping mechanism.

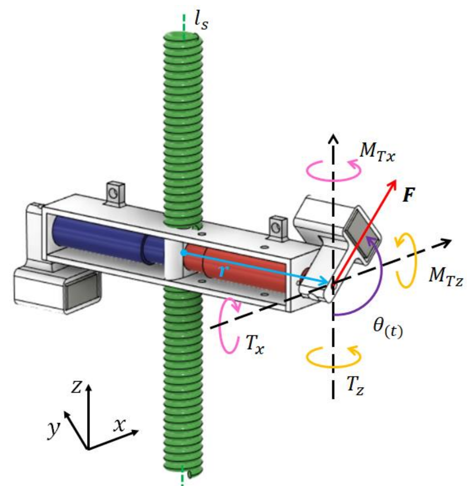

Figure 3. Turning mechanism. Force, torque, and gyroscopic moments on eccentric weight when $\theta_{(t)}$ is from $\pi/2$ to π are described.

B. Turning Design

An overview of a turning mechanism is shown in Fig. 3. Rotating only one weight at the constant speed generates a gyroscopic moment that causes turning around yaw axis, so the robot can control the direction of the jumping and posture during the movement.

Torque $\boldsymbol{T}$ that the robot receives by rotating one weight is described by (3) from combined force $\boldsymbol{F}$ of centrifugal force in (1) and gravity.

$$\boldsymbol{T} = \begin{bmatrix} T_x \\ T_y \\ T_z \end{bmatrix} = \boldsymbol{r} \times \boldsymbol{F} = \begin{bmatrix} -l(f_z - m_w g) \\ 0 \\ l f_x \end{bmatrix}, \qquad (3)$$

where $\boldsymbol{r}$ is the position vector of eccentric weights from a center point of the vibration unit, l is magnitude of $\boldsymbol{r}$, and g is the magnitude of gravitational acceleration. This torque changes the direction of eccentric weight rotation axis, generating the gyroscopic moments M_{Tx} and M_{Tz}, where M_{Tx} and M_{Tz} are gyroscopic moments generated by torque T_x and T_z, respectively. By M_{Tx} and T_z, the robot turns positively and negatively around the central axis l_s. The reason of this is following: the signs of T_x and T_z vary positive and negative depending on $\theta_{(t)}$ while rotating one weight at constant speed. The signs of T_x and M_{Tx} are coincided when viewed from the positive x- and z- axis respectively, so the sign of M_{Tx} varies positive and negative depending on the sign of T_x. The total value of T_z during one rotation of the weight is zero, the total value of T_x is positive, and M_{Tx} is also positive. Therefore, the robot turns counterclockwise when viewed from the positive z-axis. Reversing the direction of rotation of the eccentric weight causes the whole system to turn clockwise based on the same principle.

C. *Additional Components*

Outer sphere consists of PVC hemispheres with 150 mm diameters, these are assembled using poly-lactic acid (PLA) components and cellophane tape, which contributes to the robot's softness, toughness, safety. Furthermore, outer sphere has a CFRP pipe inside of φ4 mm , which is fastened to PVC hemisphere with M2 low-head screws. This pipe supports one vibration unit and two compressed springs.

III. Robot System

A. *Overview of Robot System*

Overview of the robot system is shown in Fig. 4. The robot system consists of a controller and robot. The robot can be controlled wirelessly by an operator via commands from an external computer.

B. *Electrical System*

The electrical system consists of a micro-computer unit (MCU) for control, two motor drivers for DC motors control, a wireless module for wireless operation, an IMU for posture measurement, and a power source. The components and functions of the fabricated electronic circuit are shown in Table II. The IMU is incorporated in the system for future function enhancements, and has not been used here.

C. *Control System*

The robot motions depend on position and speed of the eccentric weights assembled on each DC motor shaft. The position of each motor is controlled by proportional and derivative (PD) controller. Its target value is updated every 10 ms according to the preprogram pattern to generate rotation at the constant speed. This pattern constitutes three parameters, motion modes, interrupt time, and amount of change in target value. Motion modes are classified into continuous jumping and turning right/left in each of the target rotation speed of eccentric motors, N_{target}. Operators can control only motion modes by sending a command from a computer. Interrupt time is 10 ms for any mode, and the amount of change in target value is varied according to the motion mode.

This control method realizes continuous jumping and turning motion. It enables the positions of two eccentric weights to rotate synchronously, so the robot jumps continuously and effectively. It also enables one eccentric weight to rotate at a constant speed, so the robot turns right or left. In PD controller, incomplete derivative that adds low pass filter to D controller to reduce noise has been used. Consequently, the block diagram is shown in Fig. 5, where r is the target position value, y is the current position value of eccentric weight, e is the deviation between r and y, u is the control input value for motor, P is the controlled system (DC motor), K_p is the proportional coefficient, T_d is the derivative time, and η is the derivative coefficient and takes the value 0.1. DC motor was controlled by position tracking after determining the coefficient by step-input based on the above. As a result, the maximum value of N_{target} was 750 rpm with the two eccentric weights synchronously.

IV. Experiments and Results

The rotation speed of the eccentric motor influences jumping and turning motion of the robot. Therefore, we conducted experiments to evaluate the relationship between the motion and N_{target}. Furthermore, short delay to commands from the computer is an important factor for the robot. Therefore, we conducted experiments to evaluate whether the robot has short delay to play with children by measuring the time. Finally, we conducted experiments to evaluate motion performance of the robot in a field.

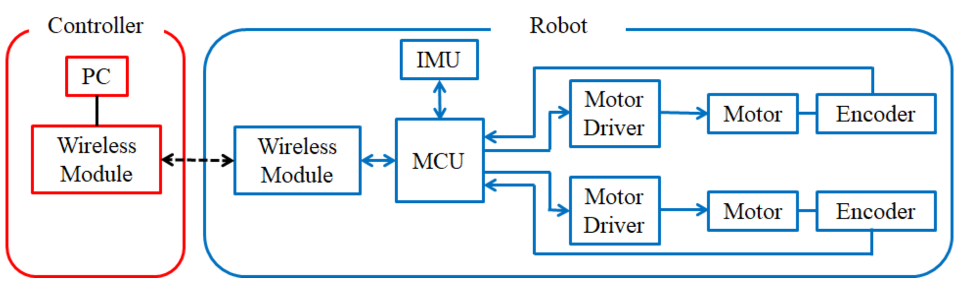

Figure 4. Overview of the robot system.

TABLE II. Components of the Electronic Circuit

Name	Function
Nucleo-F303k8	MCU
TB67H450FNG	Motor driver
XBee S2C	Wireless control
LPMS-ME1 DK	IMU
LP-3S1P360RE	Power source

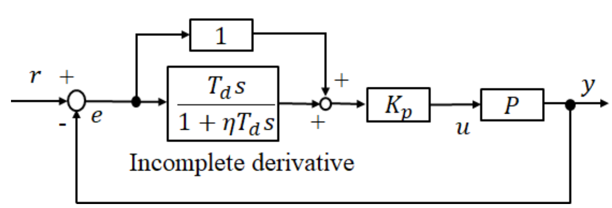

Figure 5. Block diagram.

A. Continuous Jumping

We measured the maximum jumping height in each of N_{target} by a high-speed camera (120 fps) videos recorded six times for each of N_{target}. N_{target} varied from 540 to 750 rpm in increments of 30 rpm. The videos were of the robot jumping continuously on a graph paper with a 5 mm grid. Our measurement method was as follows: first, we measured 1 scale length of the graph paper on the starting point to jump and jumping height in the video; second, we calculated the reduction percentage of the true value 5mm. Finally, we calculated the accurate jumping height from reduction percentage and the jumping height measured in the video. The mean value and standard deviation of the maximum jumping height in each of N_{target} are shown in Fig. 6, and the maximum jumping height of the robot is 15 mm. Fig. 7 shows serial photos just before the robot jumps to a maximum height at 750 rpm. These photos are from landing on the floor to maximum jumping motion of the robot. As shown in Fig. 6, the higher N_{target}, the higher the jumping height. Furthermore, Fig. 6 shows the jumping height markedly changes after 600 rpm.

B. Right/Left Turning

According to (1) and (2), rotating only one eccentric weight can cause not only turning but also jumping. Therefore, we conducted experiments under 600 rpm to cause the low jumping height based on Fig. 6. We measured the maximum average right/left turning angular velocity in each of N_{target} by a high-speed camera (120 fps) videos recorded six times for each of N_{target}. We measured the time to turn $\pi/2$ and calculated the average turning angular velocity. At 600 rpm or less, N_{target} varied from 300 to 600 rpm in increments of 75 rpm. The mean value and standard deviation of the maximum average right/left turning angular velocity in each of N_{target} are shown in Fig. 8 and Fig. 9: the higher N_{target}, the higher the average turning angular velocity up to a certain rotation speed, N_{peak}. The higher N_{target}, the lower the velocity after N_{peak}. N_{peak} is calculated by two approximate straight lines in right/left turning, respectively. Therefore, in the rotation speed for low jumping, one suitable rotation speed maximizes the average turning angular velocity.

C. System Delay

We measured the delay time from sending a command to the robot to starting motion by high-speed camera (120 fps) videos recorded six times. The videos were recorded while sending the command by a computer keyboard causing a

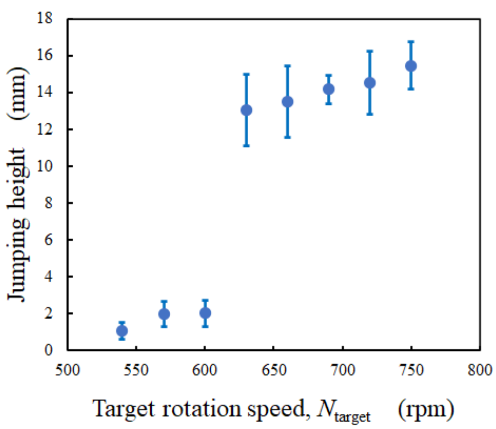

Figure 6. The relationship between N_{target} and the maximum jumping height. The error bars represent standard deviations.

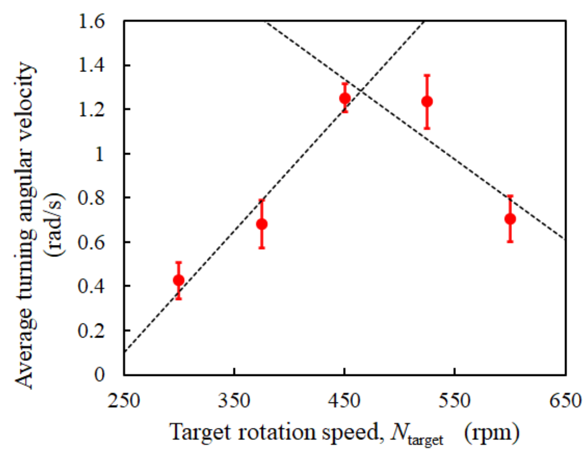

Figure 8. The relationship between N_{target} and the maximum average right turning angular velocity. The error bars represent standard deviations. Two dotted lines represent approximation straight line each three values of lower and upper. Rotational speed (N_{peak}) of the intersection point of these lines is 468.

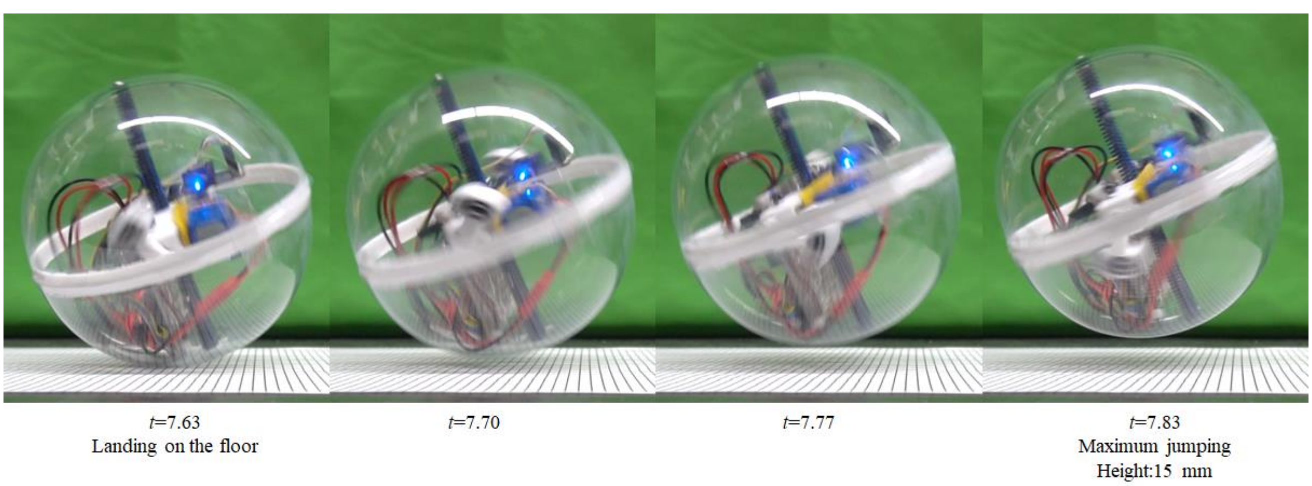

Figure 7. Serial photos from landing on the floor to maximum jumping motion of the robot. t is time from starting operation.

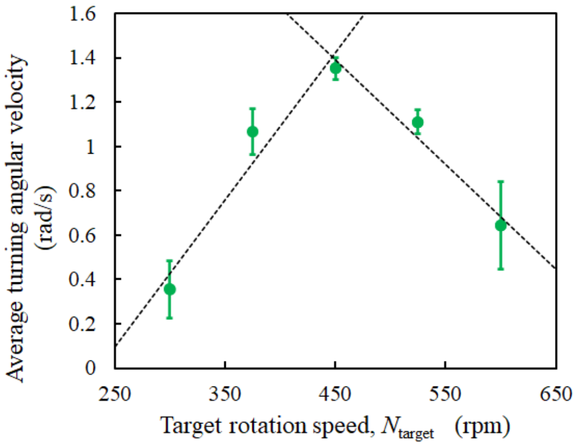

Figure 9. The relationship between N_{target} and the maximum average left turning angular velocity. The error bars represent standard deviations. Two dotted lines represent approximation straight line each three values of lower and upper. Rotational speed (N_{peak}) of the intersection point of these lines is 450.

jumping motion. The mean value and standard deviation of the delay time are shown in Table III.

D. Motion Performance

We measured a trajectory and speed of the robot while jumping continuously for one minute in a field by image processing. This field was a flat square with 1920 mm side and surrounded by pipe of φ28 mm. Fig. 10 and Fig. 11 show the results of this experiment at 0.5 seconds intervals, also the maximum and mean speed is shown in Table IV. Dots in Fig. 10 shows a position at time intervals between 0 and 60 seconds. The trajectory is shown in Fig. 10, and it is moving around. The speed is not constant but changing randomly as shown in Fig. 11. Therefore, the trajectory and speed of the robot are dynamic.

V. Discussion

A. Continuous Jumping

We confirmed that the jumping height increases with the rotation speed; the jumping height markedly changes after 600 rpm. Therefore, the jumping height of the robot can be controlled by the rotation speed of the eccentric weights. As shown in (2), the vibration force increases with rotation speed at position tracking control. It causes the spring to store elastic energy and the robot to jump higher. This tendency is the same as shown in Fig. 6. According to the maximum jumping height of 15 mm, we considered that the jumping motion is safe because the robot does not reach face-height of children and cause accidents.

Mass is the important factor in jumping. This is because a jumping force (the vibration force in this study) exceeding mass for even a moment causes jumping. The force exceeding mass several times causes jumping continuously and effectively. The vibration force exceeding the robot mass 295 g is 2.89 N. In the case of constant rotation speed of the two eccentric weights, this force is generated at 574 rpm. Therefore, the jumping height of this ball-like robot should be markedly higher above 574 rpm, but Fig.6 shows that it was markedly higher above 600 rpm, not 574 rpm. This can be

TABLE III. Delay Time

Mean value ms	22
Standard deviation ms	7.9

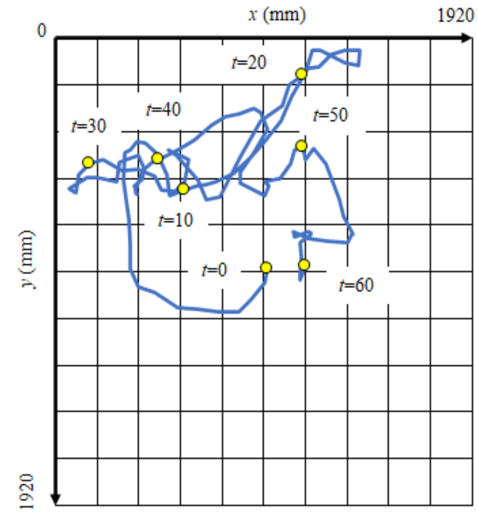

Figure 10. Trajectory of the robot in a filed. The line is trajectory. The dots are the positions of the robot at written time.

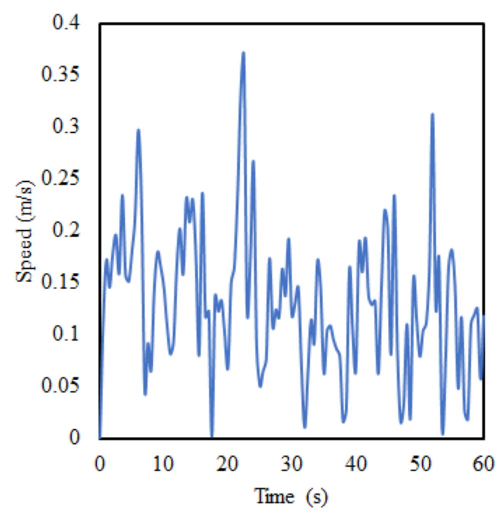

Figure 11. Speed of the robot in a filed.

TABLE IV. The Maximum and Average Speed of the Robot

Maximum value m/s	0.37
Mean value m/s	0.13

because of air resistance and reduction of jumping force by friction between vibration unit, springs, and CFRP shaft.

B. Right/Left Turning

The average right/left turning angular velocity of the robot can be controlled by the rotation speed of an eccentric weight. Under N_{peak}, low gyroscopic moment caused by small value of T_x makes friction between the robot and a floor dominant, which impacts the turning motion. Over N_{peak}, easiness to change posture of the robot by vibration impacts on turning motion. It causes runout of the turning central axis l_s and robot translational motion, so the gyroscopic moment is hard to contribute to turning around yaw axis. We concluded that one suitable rotation speed maximizes the average turning angular velocity. Turning motion is greatly affected by the robot's posture and friction between the robot and floor.

C. System Delay

The time delay by 22 ms from sending a command to starting jumping is as short as that in telexistence systems [19]. Hence, the robot has a short enough delay.

D. Proposal Application

This study proposed some applications based on the performance demonstrated in the experiment. Play with the ball-like robot can be used for free and structured play.

We considered the following play styles to execute free play. The fabricated robot is sphere in shape, so that children treat the robot as a real ball and play with it by kicking, throwing, and rolling it. Furthermore, as described in section II *A*, the robot vibrates and jumps which makes children's play enjoyable. An example of this is the way children can prevent the robot jumping and moving around by pushing the robot against a floor and feel the vibration with their body by touching the robot.

In structured play, we considered the following play styles. As described in section IV *A*, the robot jumps continuously, resulting in children and the robot dancing together. A previous study [20] suggests that synchrony in the robot's behavior influenced people's rhythmic behavior. Therefore, the jumping motion of the robot has the potential to be synchronized with children's rhythmic behavior. Furthermore, as described in section III *C*, the fabricated robot can be controlled wirelessly by an operator. A previous study [21] has also developed an autonomous interaction system using visual feedback and patterns to play with a rat robot and a mouse. Therefore, we supposed that the robot can move depending on the children's play situation by integrating it with a visual feedback system. Examples of this are the robot approaching and escaping children. As described in section IV *D*, the robot moves dynamically. This motion has the potential to attract children. Examples of this are play tag and catch ball where the robot jumps toward children.

VI. Conclusion

We reported the fabrication of the ball-like robot prototype that can jump continuously and turn right/left with wireless operation from a computer. The performance of the robot attained a maximum jumping height of 15 mm and a maximum average turning angular velocity of 1.4 rad/s. Furthermore, it can be controlled by sending a command with short delay. It has the potential to be used in free and structured play. During free play, children treat it as a real ball and generate different ways of play. During structured play, the robot induces children to move actively. The robot also has the intelligence to provide autonomous play.

References

[1] J. P. Shonkoff and A. S. Garner, "The lifelong effects of early childhood adversity and toxic stress," *Pediatrics*, vol. 129, no. 1, pp. e232-246, Jan. 2012.

[2] The LEGO Foundation, "Learning through play," UNICEF., New York, NY 10017, USA, Oct. 2018.

[3] J. Goldstein, "PLAY IN CHILDREN'S DEVELOPMENT HEALTH AND WELL-BEING," Toy Industries of Europe., Boulevard de Waterloo 36, 1000 Brussels, Feb. 2012.

[4] J. M. Zosh, E. J. Hopkins, H. Jensen, C. Liu, D. Neale, K. Hirsh-Pasek, S. L. Soils and D. Whitebread, "Learning through play: a review of the evidence," LEGO Foundation., Koldingvej 2, 7190 Billund, Denmark, Nov. 2017.

[5] P. K. Smith, *Children and Play: Understanding Children's Worlds*. USA: Wiley-Blackwell, 2009.

[6] P. Tortella, M. Haga, J. E. Ingebrigtsen, G. F. Fumagalli and H. Sigmundsson, "Comparing free play and partly structured play in 4-5-years-old children in an outdoor playground," *Front Public Health*, vol.7, Jul. 2019.

[7] K. R. Ginsburg, "The importance of play in promoting healthy child development and maintaining strong parent-child bonds," *Pediatrics*, vol. 119, no. 1, pp. 182-191, Jan. 2007.

[8] D. Bergen, K. Hutchinson, J. T. Nolan and D. Weber, "Effects of infant-parent play with a technology-enhanced toy: affordance-related actions and communicative interactions," *J. Research in Childhood Education*, vol. 24, no. 1, pp. 1-17, 2009.

[9] F. Michaud, J. Laplante, H. Larouche, A. Duquette, S. Caron, D. Letourneau, and P. Masson, "Autonomous spherical mobile robot for child-development studies," in *IEEE Transactions on Systems, Man, and Cybernetics – Part A: Systems and Humans*, vol. 35, no. 4, pp. 471–480, July 2005.

[10] S. Golestan, P. Soleiman and H. Moradi, "Feasibility of using sphero in rehabilitation of children with autism in social and communication skills," *2017 International Conference on Rehabilitation Robotics (ICORR)*, London, UK, 2017, pp. 989-994.

[11] Y. Takeda, S. Baba, P. Ravindra S De Silva, and M. Okada, "COLUMN: discovering the user invented behaviors through the interpersonal coordination," *in Proc. 17th Int. Conf. Human-Computer Interaction*, 2015, pp. 787-796.

[12] M. B. Parten, "Social participation among pre-school children," *J. Abnormal and Social Psychology*, vol. 27, pp. 243-269, 1932.

[13] M. H. Raibert, H. B. Brown Jr, and M. Chepponis, "Experiments in balance with a 3D one-ledded hopping machine," *Int. J. Robotics Research*, vol. 3, no. 2, pp. 75-92, 1984.

[14] S. H. Hyon, and T. Mita, "Development of a biologically inspired hopping robot-"Kenken"," in *Proc. 2002 IEEE Int. Conf. Robotics and Automation (Cat. No.02CH37292)*, Washington, DC, USA, 2002, pp. 3984-3991 vol.4.

[15] J. Zhao, N. Xi. B. Gao, M. W. Mutka, and L. Xiao, "Development of a controllable and continuous jumping robot", *2011 IEEE Int. Conf. Robotics and Automation*, Shanghai, China, 2011, pp. 4641-4619.

[16] X. Yu and F. Iida, "Minimalistic Models of an Energy-Efficient Vertical-Hopping Robot," in *IEEE Trans. Industrial Electronics*, vol. 61, no. 2, pp. 1053-1062, Feb. 2014.

[17] D. KAJI, J. TANAKA, and Y. TAGAWA, "Development of a self-excited jumping robot with eccentric weights," in *Proc. JSME annual Conf. on Robotics and Mechatronics (Robomech in Japanese)*, vol. 14, no. 2, 2014.

[18] K. Nagaoka and K. Yoshida, "Modeling and analysis of ciliary micro-hopping locomotion actuated by an eccentric motor in a microgravity," *2013 IEEE/RSJ Int. Conf. Intelligent Robots and Systems*, Tokyo, Japan, 2013, pp. 763-768.

[19] S. Sasaki and T. Okazaki, "Feasibility study for telexistence on a ship - measurement of delay time of satellite communication," *2016 IEEE Int. Conf. Systems, Man and Cybernetics (SMC)*, Budapest, Hungary, 2016, pp. 001477-001482.

[20] M. P. Michalowski, S. Sabanovic, H, Kozima, "A dancing robot for rhythmic social interaction," *2007 2nd ACM/IEEE Int. Conf. Human-Robot Interaction (HRI)*, Arlington, VA, USA, 2007, pp. 89-96.

[21] H. Ishii, M. Nakasuji, M. Ogura, H. Miwa and A. Takanishi, "Experimental Study on Automatic Learning Speed Acceleration for a Rat using a Robot," in *Pro. 2005 IEEE Int. Conf. Robotics and Automation*, Barcelona, Spain, 2005, pp. 3078-3083.